International Journal of Engineering & Technology, 7 (4.14) (2018) 560-564

International Journal of Engineering & Technology

Website: www.sciencepubco.com/index.php/IJET

Research paper

Photosensitization of TiO_2 Nanotube Arrays with Nanocrystalline Pbs

Ying-Chin Lim[1]*, Nurul Munirah Hamdan[1], Nur Farah Atikah Harun[1], Lim Ying Pei[2]

[1]*Faculty of Applied Sciences, Universiti Teknologi MARA, 40450 Shah Alam, Selangor, Malaysia*
[2]*Faculty of Chemical Engineering, Universiti Teknologi MARA, 40450 Shah Alam, Selangor, Malaysia*
**Corresponding author E-mail: limyi613@salam.uitm.edu.my*

Abstract

Narrow bandgap lead sulfide (PbS) nanoparticles, which may expand the light absorption range to visible region, have attracted tremendous interest serving as promising sensitizer in coupled semiconductor for photoelectrochemical cell. In this study, PbS were deposited onto titania nanotubes by successive ionic layer adsorption and reaction (SILAR) method. During the SILAR deposition, the growth of PbS onto titania nanotubes (PbS/TNT) had been tuned by tailoring the concentration of the precursor solution. The sample microstructure was characterized using Energy Dispersive X-Ray (EDX), Field Emission Scanning Electron Microscopy (FESEM) and X-Ray Diffraction (XRD). By varying the concentration of precursor solution, size and distribution of PbS nanoparticles could be tuned. Upon growth of PbS onto TNT, all samples showed enhanced photocurrent response ascribed to the changes in microstructure and optical properties of the synthesized samples. At 100 mM solution concentration dipped for 5 SILAR cycles, the sample demonstrated the highest peak photocurrent density of 890 μA/cm^2 and a corresponding photoconversion efficiency of 0.55% compared to the as-prepared TNT (36 μA/cm^2). The PbS/TNT composite could be considered as an excellent photoelectrode material applied in the solar conversion devices due to its high visible light harvesting capability.

Keywords: *Morphology; Photoelectrochemical; Photocurrent; Titania Nanotubes; SILAR.*

1. Introduction

Bulk titania (TiO_2) has low quantum efficiency by means, having high charge carriers' recombination rates. Both optimal material and proper architecture are essential to limit the recombination of photoinduced charge carriers. Furthermore, bulk TiO_2 has lower surface area due to its large size and thus limits its application. To overcome this problem, TiO_2 nanotube (TNT) is favorable due to its small size and hollow structure that can greatly increase the active surface area and enhance the efficiency of its application as photocatalyst for wastewater treatment [1]. In addition, TNT fabricated via electrochemical anodization of Ti has oriented pathway that is believed to aid in charge transfer between interfaces. Meanwhile, TiO_2 nanoparticles, though having high surface area and surface energy, usually incur a high cost after water treatment process as filtration is necessary to remove the suspended solid. The nanoparticles also tend to agglomerate easily and it is also difficult to separate or recover the used TiO_2 from the treated water and resulted in re-pollution [2,3]. It is reported that a thin film of TiO_2 nanotube is much favorable instead as no post-treatment is needed. In addition, the low surface area of TiO_2 as a result from the thin film form could be overcome by using high surface area hollow nanotubes form [4].

Among lots of semiconductors (ZnO, TiO_2, ZrO_2, WO_3) that have been investigated for photocatalytic reaction, TiO_2 nanomaterial is one of the most promising candidates due to its chemical stability, low cost, abundant and non-toxicity [5]. However, TiO_2 is a large band gap semiconductor that can only be excited under the ultraviolet irradiation resulting in low utilization of solar energy. Meanwhile, the photo-generated electrons and holes in TiO_2 recombine quickly leading to a low quantum efficiency [6]. Anatase phase and rutile phase of TiO_2 has a large bandgap of 3.2 eV and 3.0 eV respectively [7]. Sensitization of TiO_2 with narrow band gap materials is believed to extend the absorption spectra of TiO_2 towards visible light region and thus make full use of solar radiation. As such, successive ionic layer adsorption and reaction (SILAR) method is used in this study to deposit a narrow band gap metal chalcogenide, PbS onto the TiO_2 nanotube. PbS is one of the promising sensitizers due to its low band gap of about 0.41 eV which can allow extension of the absorption band toward the near infrared part of the solar spectrum [8-11]. The SILAR method is reported to be advantageous as compared to other deposition methods such as chemical bath deposition and electrodeposition due to its ability to deposit on both the inner and outer wall of nanotubes [8]. Furthermore, PbS is insoluble thus it is a less toxic forms of lead than others. A work by Rhana et al. reported that the SILAR cycle play an important role to tune the photocatalytic and photovoltaic properties of titania sensitised with PbS by monitoring the degradation of methylene blue under visible light irradiation [6]. Therefore, the present work aims to investigate the other experimental parameter i.e. the effects of precursor solution concentration on the formation and structure of PbS deposit on titania (PbS/TNT) and their photoelectrochemical performance. A previous work by Zhang et al. (2016) demonstrated that the deposition of PbS had resulted in change of sample surface roughness and subsequently modified the band gap structure, flat band potential, lifetime and transport of the photo-induced charge carriers [12].

2. Materials and methods

2.1. Synthesis of PbS sensitized TiO_2 nanotube array

PbS/TNT was synthesized via a two-step anodization SILAR method. Firstly, TNTs were prepared by anodization of Ti foils in a two-electrode electrochemical cell containing 0.5 wt% NH_4F, ethylene glycol and glycerol (1:1 ratio). The anodizing conditions were set at 20 V for 30 mins. A heat treatment was performed at 500 ^oC for 2 hours to transform the amorphous TNT into anatase form. Subsequetly, PbS nanoparticles were deposited onto TNTs by SILAR approach which were similar to our previous work [13]. Typically, $Pb(NO_3)_2$ solution was used as cationic precursor and Na_2S solution was used as the anionic precursor. During the SILAR process, TNT was first immersed into 0.02 M $Pb(NO_3)_2$ solution for 5 minutes to allow Pb^{2+} to adsorb onto TNT. This was followed by rinsing TNT with distilled water for 1 minute to remove the unabsorbed ions before dipping again the TNT into 0.02 M Na_2S solution for another 5 minutes. The process was then followed by rinsing the TNT with distilled water again for 1 minute to complete one full cycle of operation. In this study, the SILAR process was repeated for 5 cycles and the concentration of the precursor solution was varied between 5 to 200 mM. Subsequently, the PbS/TNT was kept in desiccator before further characterization.

2.2. Characterization

The morphology of the samples was characterized by a field emission scanning electron microscope (FESEM, Carl Zeiss SUPRA 40 VP). Quantitative analysis of elements was carried out with Energy Dispersive X-ray Spectrometer attached with FESEM. The crystalline structure of the samples was identified using a X-ray Diffractometer (X'Pert Pro-MPD, PANalytical) operating at 40 kV using Cu Kα (λ = 1.504Å). The optical absorbance behaviour of TNT and PbS/TNT was characterized using UV-VIS-NIR spectrophotometer (Model: UV-3600, Shimadzu Corporation, Kyoto, Japan). The wavelength was scanned from 200 nm to 800 nm with $BaSO_4$ was used as the reflectance standard. For photoelectrochemical measurements, a 100 mL rectangular quartz cell was used. Typically, a three–electrode configuration which composed of the as-prepared sample as the working electrode, a platinum wire as the counter electrode, a Ag/AgCl as the reference electrode and 0.1 M Na2S as an electrolyte. The working electrode was illuminated with a 300 W halogen lamp and the photocurrent was recorded by a potentiostate (Autolab) during a potential sweep from +1 to –1 V.

3. Results and discussion

In this study, TNT was prepared by electrochemical anodization of Ti followed by deposition of PbS onto the calcined TNT film via SILAR method producing PbS/TNT. Figure 1 shows the changes in colour of films after each step. The colour changes from silver for blank Ti and subsequently getting darker after the anodization process. After calcination at 500^oC for 2 hours, the colour of film changed to dark blue indicates that crystallinity of TNT was successfully induced. Finally, the colour turned to black after the deposition of PbS onto TNT, suggesting that coupling of TiO_2 with PbS is a successful one as PbS is black in nature.

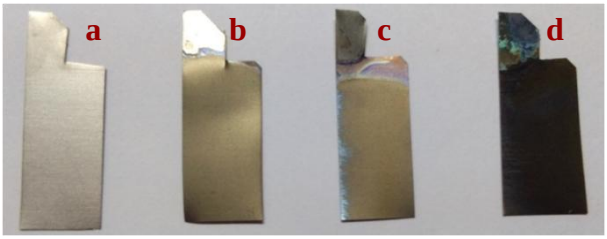

Fig.1: The appearance of sample a) blank Ti b) as-anodized TNT c) calcined TNT d) PbS/TNT

The distribution and size of the PbS particles were tuned by varying the concentration of lead and sulfur precursor solution during the SILAR process. The concentration of $Pb(NO_3)_2$ and Na_2S solutions was varied between 5 mM, 10 mM, 100 mM and 200 mM. The immersion time of TNT in the solutions and the dipping cycle were fixed to 5 minutes and 5 cycles, respectively. Figure 2 shows the FESEM images of PbS/TNTs morphologies prepared at different concentration of $Pb(NO_3)_2$ and Na_2S solutions.

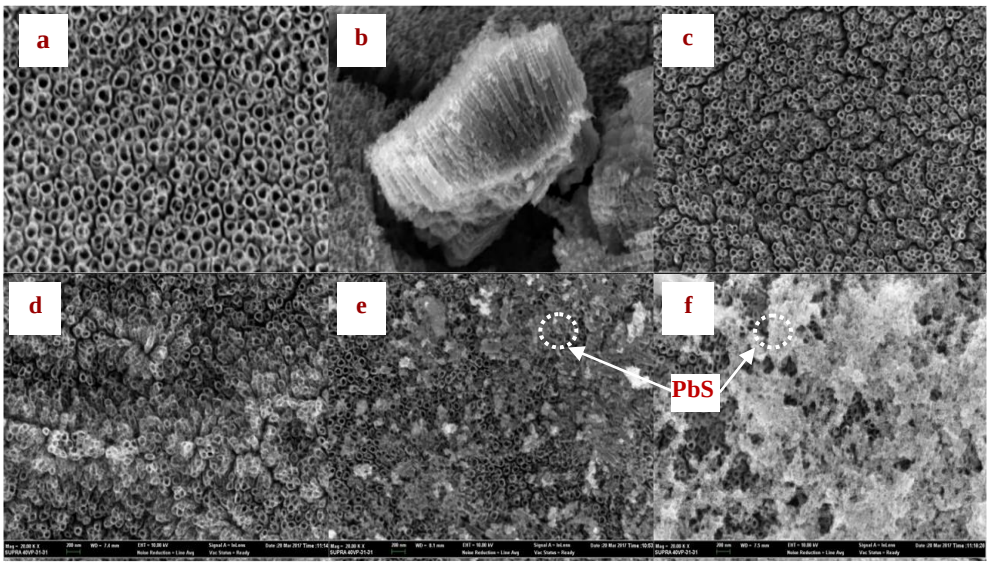

Fig.2: FESEM images for a) calcined TNT b) cross sectioval view of calcined TNT and PbS/TNT prepared at various solution concentrations of c) 5 mM d) 10 mM e) 100 mM and f) 200 mM

Figure 2a shows the FESEM image of a well- organized TNT with opened tube mouth. Figure 2b shows that the tubes were in the regular vertical alignment with ripples on their side walls. Furthermore, TiO_2 ridges that formed between the nanotubes resulted in the self organized TNT. These interconnected ridges are important in transporting the photoinjected electron to the Ti substrate [14]. It is expected that phase change from amorphous TiO_2 to anatase upon calcination is crucial for a better nanostructure arrangement of the nanotubes. Formation of highly ordered and vertically oriented nanotubes is clearly revealed from the cross-

sectional FESEM image (Figure 2b). The length of nanotubes is approximately 520 nm. All PbS/TNT samples were vertically oriented and well aligned. It is observed that the amount of PbS onto TNT increases with the increasing of solution concentration. At 5 and 10 mM, the nanotubes still retained their morphology with no discernible changes in the tube diameter. On increasing to 100 mM, more obvious PbS nanoparticles (NPs) were deposited on the surface of nanotubes. Although non-homogenous deposition of PbS onto TNT was obtained, one can observe that the PbS is not covering the top entrance of the tube. However, high concentration of PbS will result in too fast formation of PbS NPs on the surface of TNTs and it is not favorable as NPs tend to agglomerate forming large particles. In this study, the surface of TNTs is mostly covered with PbS when the concentration was increased to 200 mM as shown in Figure 2(f) and this may not be good for the photoelectrochemical performance [15]. It is believed that both PbS and TNTs could contribute together in the generation of photocurrent. As such, photon absorption by TNTs might be disrupted as the PbS covered almost entire surface of TNTs.

EDX analysis was used to determine the elemental composition of the samples. Table 1 shows the amount of each element in the blank Ti, pure TNTs and PbS/TNTs prepared at 100 mM solution concentration.

Table 1: Elemental composition for Ti, TNT and PbS/TNT

Sample	Atomic percent (%)			
	Ti	O	Pb	S
Blank Ti	100.0	-	-	-
Pure TNT	58.13	41.87	-	-
PbS/TNT	42.14	56.01	0.89	0.96

For blank Ti sample, 100% of Ti presents in the sample and no other impurities were detected. After anodization, the elements of Ti and O were detected due to the formation of TiO_2 nanotube. This explained the high amount of O in the pure TNT compared to the blank Ti. Upon immersion in SILAR precursor solution, Pb and S could be detected for PbS/TNT sample, indicating that PbS NPs were successfully deposited onto TNTs. The atomic ratio of Pb and S is almost 1:1 suggesting the formation of stoichiometry ratio of PbS.

The crystallinity and phase formation of samples were examined by XRD. Figure 3 shows the XRD patterns of as-anodized TNT, calcined TNT as well as PbS/TNT prepared at various concentrations. The dipping cycle and immersion time were constant at 5 cycles and 5 minutes respectively. The diffraction of Ti peaks can be observed at 2θ = 35.1°, 38.4°, 40.2°, 53.0°, 62.9°, 70.6° and 76.2° (JCPDS 44-1294) respectively for as-anodized TNT and no anatase/rutile phase was observed and this indicates the amorphous nature of TNT. Upon calcination, TNT crystallizes forming anatase phase at 2θ = 25.4° and 48.0° (JCPDS 21-1272), diffraction peaks were very intense indicating the high crystallinity of TNT. The samples were annealed at 500°C for 2 hours to improve the crystallinity. After deposition of PbS onto TNT, new diffraction peaks of PbS were observed at 2θ = 25.9°, 30.1° and 43.0° (JCPDS 65-0307). It can be observed that the intensity of PbS peak increases with the increased of SILAR concentration. This provides powerful evidence for the successful deposition of PbS onto TNT.

Three-electrode photoelectrochemical cell was used to evaluate the PEC performance of the prepared PbS/TNT photoelectrode. The photoelectrochemical behavior of the samples was evaluated by chopping the light irradiated from a halogen lamp (intensity of 150 mW/cm^2) at a constant frequency in 0.5 M of Na_2SO_4 as supporting electrolyte so that both the dark and photocurrent can be obtained in a single experiment. The current range was set at 10 mA while the scan rate was set at 0.05 V/s from +1V to -1V. Photocurrent recorded at 0.3 V vs. Ag/AgCl was used to calculate the photoconversion efficiency. A graph of current density against potential (vs. Ag/AgCl) was plotted to identify the sample with the highest photoconversion efficiency. Figure 4 shows the comparison of photocurrent-potential curve response for PbS/TNT prepared at various concentrations.

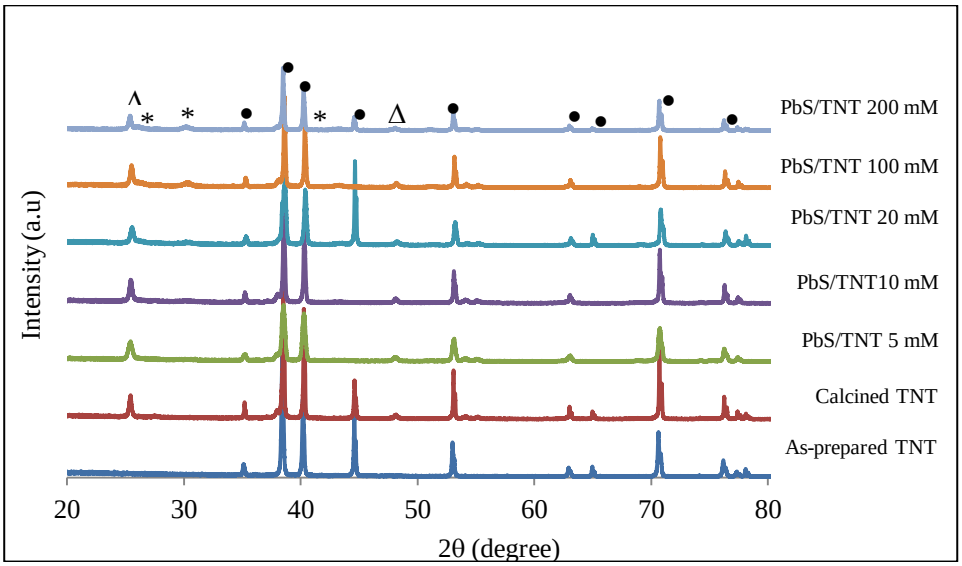

Fig. 3: XRD patterns of as-prepared TNT, calcined TNT and PbS/TNT prepared at different concentration with Δ, * and • represents anatase, PbS and titanium respectively.

As can be seen from Figure 4, all samples showed flat baseline response in the dark condition, suggesting good coverage of sample on the Ti foil and demonstrated a good quality of film. Current density for all samples increases as the light is switched on, and drops to zero as soon as the light is cut off, indicating very fast photoelectrochemical response of the samples across potential. Pure TNT shows relatively low photocurrent response and upon deposition of PbS, a higher photocurrent response was observed for all PbS/TNT samples. A higher photocurrent response demonstrated by PbS/TNT could also mean a lower electron-hole recombination and higher photoelectron transfer efficiency, which could eventually benefit a photocatalytic reaction. This provides powerful evidence that coupling TNT with PbS, which acts as sensitizer can enhance its photoelectrochemical performance. Apparently, the photocurrent increased by 0.52% with increasing concentration from 5 mM to 100 mM. However, the photocurrent start to decline when the concentration was further increased to 200 mM. When

approaching 0 V vs. Ag/AgCl, the dark current and photocurrent start to drop slowly.

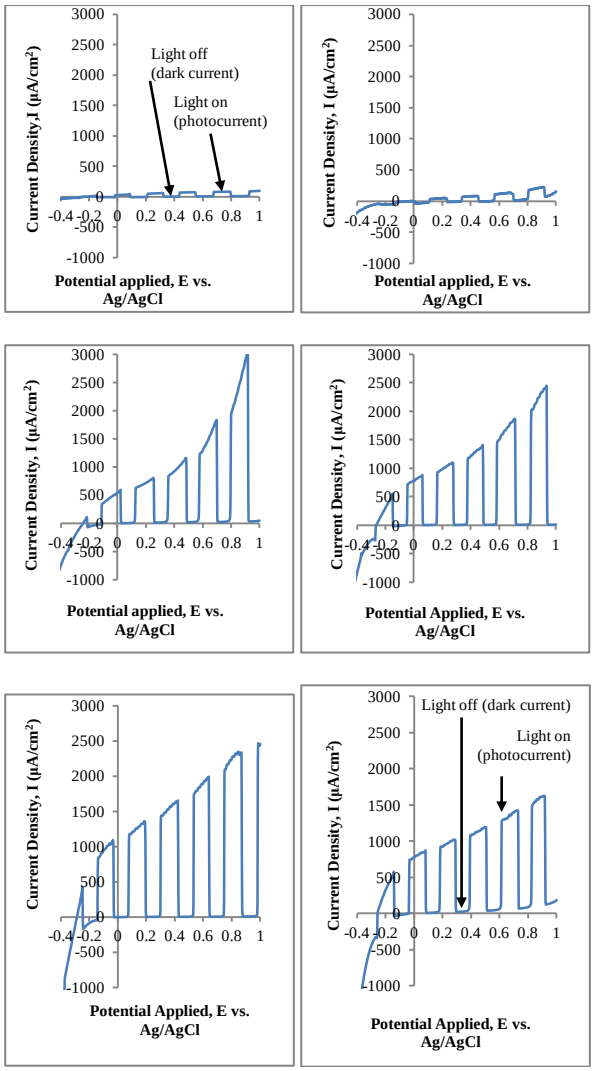

Fig. 4: Current density of (a) pure TNT and PbS/TNT prepared at various concentrations (b) 5 mM (c) 10 mM (d) 20 mM (e) 100 mM (f) 200 mM.

Table 2 shows the photoconversion efficiency calculated for each samples at different SILAR concentration. As expected, All PbS/TNT samples prepared at different SILAR concentrations exhibited higher photoconversion efficiency compared to the pure TNT which only possess 0.023 % efficiency at 0.3 V (vs. Ag/AgCl). PbS/TNT prepared at 100 mM shows a 24-fold increased in photocurrent density which resulted in the highest photoconversion efficiency of 0.55% at 0.3 V (vs. Ag/AgCl) compared to the pure TNT. As can be seen in FESEM image in Figure 2(e), high amount of PbS NPs were observed on the surface of TNTs which induced a higher current density. A study reported by Du et al. (2018) demonstrated that PbS might act light absorbers to accelerate electron-hole separation and transport [16]. At 200 mM, the photoconversion efficiency starts to decrease probably due to the agglomeration and oversized particles of PbS as shown in FESEM image in Figure 2(f). Excess deposition of PbS onto TNT can act as barrier for charge transfer. Therefore, PbS/TNT prepared at SILAR concentration of 100 mM has the highest efficiency to absorb more photon, resulting in high ability of PbS/TNT to convert the light energy to generate current. UV-DRS analysis was carried out to support our results obtained from the PEC measurement. Figure 5 shows the comparison of absorption spectra for pure TNT and PbS/TNT sample.

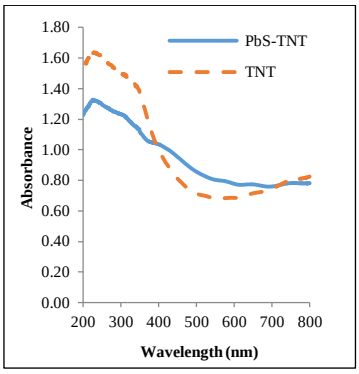

Fig. 5: Absorption spectrum of pure TNT and PbS/TNT

From the UV spectra, the estimated band gap for pure TNT is 3.0 eV, consistent with the typical value for TiO_2. For PbS/TNT, the sample showed no sharp transition of absorbance probably due to very small band gap of PbS (0.44 eV). Therefore, the band gap of the synthesized PbS/TNT in this study could not be determined. However from the UV-DRS analysis, PbS/TNT showed a much stronger absorption in the visible region (500-700 nm) compared to the pure TNT, suggesting that PbS/TNT could serve as a better visible-light responsive photoanode compared to pure TNT. Meanwhile pure TNT absorbed much stronger in the UV region (200-400 nm). This analysis supports the PEC result that sensitization of TNT with PbS resulted in higher photocurrent ascribed to high absorption in the visible light region.

Table 2: Photocurrent density and photoconversion efficiency calculated for PbS/TNT prepared at various concentrations and pure TNT

Sample	Average Photocurrent Density (A/cm^2)	Photoconversion Efficiency (η%)
Pure TNT	3.6×10^{-5}	0.023
PbS/TNT 5 mM	5.2×10^{-5}	0.032
PbS/TNT 10 mM	5.3×10^{-4}	0.33
PbS/TNT 20 mM	6.8×10^{-4}	0.42
PbS/TNT 100 mM	8.9×10^{-4}	0.55
PbS/TNT 200 mM	6.2×10^{-4}	0.39

In order to analyze the stability of PbS/TNT photoanode, chronoampererometry measurement was conducted. Figure 6 provides the characteristics of the photocurrent density against time for PbS/TNT under 0 V bias and 0.3 V vs. Ag/AgCl reference electrode. When the light was irradiated from a halogen lamp, all samples showed an immediate change in current. The photocurrent of the samples drops to zero as soon as the light was chopped, indicating fast response of PbS/TNT sample. From Figure 6, it can be observed that the photocurrent density is decreasing with time for PbS/TNT. The photocurrent density is the lowest during the third run of the PEC test at 0.3 V (vs. Ag/AgCl) as shown in Figure 6(d). This suggest that PbS/TNT shows a low resistance to photocorrosion. This can be attributed to the dissolution of PbS during PEC test, desorption of ions of Na_2SO_4 electrolyte from the surface of PbS/TNT which leads to decrease in PEC performance of the samples over time. Moreover, the chemical change of the PbS NPs and the hole-induced self-oxidative decomposition of the metal chalcogenide also cause the photoelectochemical performance of the samples to decrease upon light illumination [17]. In order to improve the PEC performance of PbS/TNT, Na_2SO_4 electrolyte was purged by using nitrogen gas for 5 minutes to remove oxygen from the solution. The reason why nitrogen gas was selected is due to the fact that it is relatively inert as it is neither reacts with the solution nor the carries moisture. It is also inexpensive and can be purified. The purpose of removing oxygen from the solution is to prevent the formation of PbO which will reduce the PEC performance. As can be seen from Figure 6(e), the performance of PbS/TNT after purging in nitrogen shows a tremendous increase in photocurrent, although one can still observe a decrease in photocurrent over time.

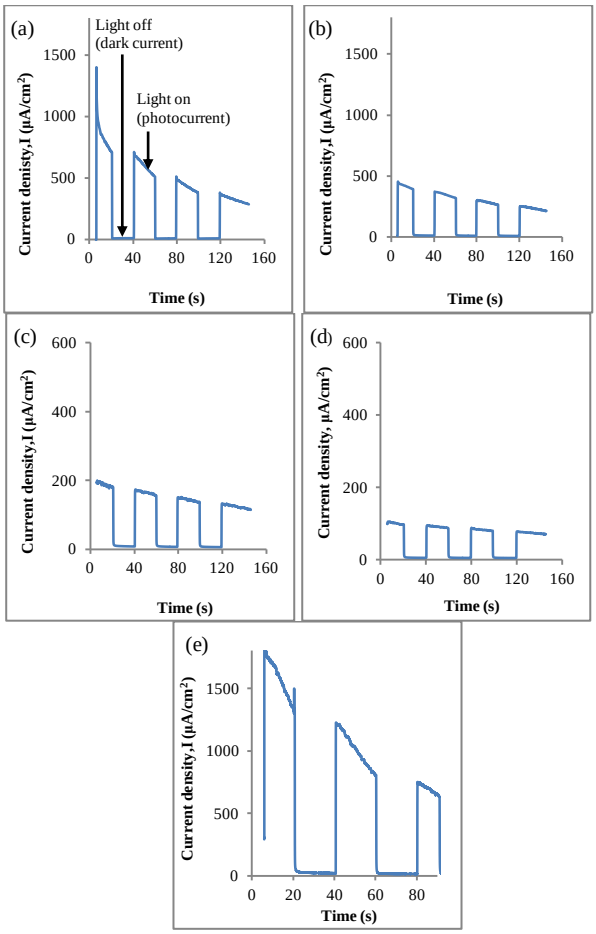

Fig. 6: Phototransients measurement from halogen lamp with 20s light pulse of PbS/TNT run at (a) 0 V (b) 0.3 V first run (c) 0.3 V second run (d) 0.3 V third run (e) 0.3 V purged under nitrogen. All potential quoted w is against Ag/AgCl.

4. Conclusion

In summary, a fast and simple SILAR method has been presented in this work to deposit PbS onto titania nanotubes and the formation of PbS/TNT was confirmed by XRD, EDX and FESEM. An aqueous solution of 100 mM of both the cationic and anionic precursor solution was found to be the optimum solution to prepare PbS/TNT. The sensitized PbS/TNT demonstrated a 23-fold improvement in photocurrent, as compared to pure TNT counterpart. The changed in microstructure and optical behaviour of the prepared PbS/TNT sample leading to the enhancement of photoelectrochemical performance. Nevertheless, PbS/TNT suffers from photo corrosion due to leaching of PbS from TNT and reduces the overall photoconversion efficiency.

Acknowledgement

The authors would like to thank Faculty of Applied Sciences, UiTM Shah Alam for the facilities provided. This work is financially supported by the Ministry of Education Malaysia via the FRGS grants (FRGS/1/2017/STG07/UITM/03/4) and Universiti Teknologi MARA, Shah Alam internal GIP grant (600-IRMI 5/3/GIP (025/2018).

References

[1] Paramasivam, I., Jha, H., Liu, N., & Schmuki, P. (2012). A review of photocatalysis using self-organized TiO_2 nanotubes and other ordered oxide nanostructures. *Small*, *8*(20), 3073-3103.

[2] Crişan, M., Drăgan, N., Crişan, D., Ianculescu, A., Niţoi, I., Oancea, P., Todan, L., Stan, C. & Stănică, N. (2016). The effects of Fe, Co and Ni dopants on TiO_2 structure of sol–gel nanopowders used as photocatalysts for environmental protection: A comparative study. *Ceramics International*, *42*(2), 3088-3095.

[3] Bethi, B., Sonawane, S. H., Bhanvase, B. A., & Gumfekar, S. P. (2016). Nanomaterials-based advanced oxidation processes for wastewater treatment: a review. *Chemical Engineering and Processing: Process Intensification*, *109*, 178-189.

[4] Marien, C. B., Cottineau, T., Robert, D., & Drogui, P. (2016). TiO_2 nanotube arrays: influence of tube length on the photocatalytic degradation of paraquat. *Applied Catalysis B: Environmental*, *194*, 1-6.

[5] Dvoranova, D., Brezova, V., Mazúr, M., & Malati, M. A. (2002). Investigations of metal-doped titanium dioxide photocatalysts. *Applied Catalysis B: Environmental*, *37*(2), 91-105.

[6] Rahna, N. B., Kalarivalappil, V., Nageri, M., Pillai, S. C., Hinder, S. J., Kumar, V., & Vijayan, B. K. (2016). Stability studies of PbS sensitised TiO_2 nanotube arrays for visible light photocatalytic applications by X-ray photoelectron spectroscopy (XPS). *Materials Science in Semiconductor Processing*, *42*, 303-310.

[7] Low, J., Cheng, B., & Yu, J. (2017). Surface modification and enhanced photocatalytic CO_2 reduction performance of TiO_2: A review. *Applied Surface Science*, *392*, 658-686.

[8] Ullah, K., Meng, Z. D., Ye, S., Zhu, L., & Oh, W. C. (2014). Synthesis and characterization of novel PbS–graphene/TiO_2 composite with enhanced photocatalytic activity. *Journal of Industrial and Engineering Chemistry*, *20*(3), 1035-1042.

[9] Luo, Y., Dong, C., Li, X., & Tian, Y. (2015). A photoelectrochemical sensor for lead ion through electrodeposition of PbS nanoparticles onto TiO_2 nanotubes. *Journal of Electroanalytical Chemistry*, *759*, 51-54.

[10] Zhang, Z., Shi, C., Chen, J., Xiao, G., & Li, L. (2017). Combination of short-length TiO_2 nanorod arrays and compact PbS quantum-dot thin films for efficient solid-state quantum-dot-sensitized solar cells. *Applied Surface Science*, *410*, 8-13.

[11] Zhou, R., Huang, Y., Wan, L., Niu, H., Ji, F., & Xu, J. (2017). Constructing aligned single-crystalline TiO_2 nanorod array photoelectrode for PbS quantum dot-sensitized solar cell with high fill factor. *Journal of Alloys and Compounds*, *716*, 162-170.

[12] Zhang, X., Wang, B., & Liu, Z. (2016). Tuning PbS QDs deposited onto TiO_2 nanotube arrays to improve photoelectrochemical performances. *Journal of Colloid and Interface Science*, *484*, 213-219.

[13] Harun, N. F. A., Mohd, Y., Lim, Y. P., Yin, C. Y., & Lim, Y. C. (2018). Understanding the characteristics, enhanced optical and photoelectrochemical performance of copper-loaded titania nanotubes synthesized via successive ionic layer adsorption reaction. *Journal of Materials Science: Materials in Electronics*, *29*(16), 14210-14221.

[14] Lim, Y. C., Zainal, Z., Tan, W. T., & Hussein, M. Z. (2012). Anodization parameters influencing the growth of titania nanotubes and their photoelectrochemical response. *International Journal of Photoenergy*, *2012*.

[15] Ayal, A. K., Zainal, Z., Lim, H. N., Talib, Z. A., Lim, Y. C., Chang, S. K., & Holi, A. M. (2017). Photocurrent enhancement of heat treated CdSe-sensitized titania nanotube photoelectrode. *Optical and Quantum Electronics*, *49*(4), 164.

[16] Du, K., Liu, G., Chen, X., & Wang, K. (2018). Fast charge separation and photocurrent enhancement on black TiO_2 nanotubes co-sensitized with Au nanoparticles and PbS quantum dots. *Electrochimica Acta*, *277*, 244-254.

[17] Zhou, C., Geng, Y., Chen, Q., Xu, J., Huang, N., Gan, Y., & Zhou, L. (2016). A novel PbS/TiO2 composite counter electrode for CdS quantum dot-sensitized ZnO nanorods solar cells. *Materials Letters*, *172*, 171-174.